

# Study and design of a patch antenna for biomedical applications

Younes Siraj<sup>1\*</sup>, Kaoutar S. Alaoui<sup>2</sup>, and Jaouad Foshi<sup>1</sup>

<sup>1</sup>ERTTI: Laboratory of Renewable Energies, Processing and Transmission of Information, Faculty of Sciences and Techniques Errachidia, Moulay Ismail University Meknes, Morocco

<sup>2</sup>EIDD: Engineering and Sustainable Development Research Team, Dakhla Higher School of Technology, Ibn Zohr University, Morocco

**Abstract.** This work presents the performance of a Dual-band patch antenna with L-shaped slot for biomedical applications. The antenna works at 2.4 GHz and 3.33 GHz. A semi-flexible substrate material which is "Taconic TLX (tm)" with a relative dielectric constant,  $\epsilon_r$  of 2.55, loss tangent,  $\tan \delta$  of 0.0019 and thickness,  $h$  of 0.7 mm has been proposed to be the isolant element of the antenna. The size of the antenna is 60 x 55 mm<sup>2</sup>. The slots in the rectangular radiating patch were introduced to produce the resonant frequencies of 2.4GHz and 3.33GHz. The simulations of the microstrip patch antenna shows the reflection coefficient,  $S_{11}$  of -31.67 dB and -20.25 dB at 2.4 GHz and 3.27 GHz respectively. The proposed antenna shows a peak gain of 5.01 dB at 2.4 GHz. The results were obtained using HFSS (high frequency structured simulator) software.

**Keywords:** *Microstrip patch antenna, Dual-Band antenna, Defected Ground Structure (DGS), Biomedical applications, L-Shaped, slotted patch, HFSS.*

## 1. Introduction

Over the past few decades, wireless communication has witnessed a great development and become an integral part of our daily lives. With the ever-increasing demand for higher data rates and more efficient communication systems, the development of antennas that can operate over multiple frequency bands with a small size has become increasingly important. In general, the patch antennas are simple and compact that are widely used in many applications, such as wireless communication systems [1], biomedical field [2], 5G applications [3], Wi-Fi & Wi-Max Applications [4]- [5], due to their low profile, ease of integration, high efficiency and low fabrication price.

Dual-band patch antennas have the added advantage of being able to operate over two frequency bands, making them ideal for biomedical applications that require multi-band operation, such as implantable medical devices, remote monitoring systems, and wearable sensors. These applications require antennas that can operate over multiple frequency bands

---

\* Corresponding author: [y.siraj@edu.umi.ac.ma](mailto:y.siraj@edu.umi.ac.ma)

to support the transmission of various types of data, from low-frequency physiological signals to high-speed digital data. This type of antenna has gained popularity in recent years. [6] present a flexible and wearable dual band bio-based antenna for WBAN applications. In [7] a novel dual-band wearable antenna using Rectangular Parasitic Elements (RPEs) and Defected Ground Structure (DGS) for tele-monitoring applications. A Low-profile dual-band implantable antenna for compact implantable biomedical devices is proposed in [8]. [9] present a planar CPW fed dual ring antenna with DGS is designed to work in the WLAN bands. In [10] A new dual-band antenna for energy harvesting application, it works at 2.4 GHz and 5.4 GHz. An Analysis and Design of E-Shaped Dual-frequency Microstrip Antenna Based on CPSO Algorithm is given in [11]. [12] propose a Design of Directional Two L shaped Microstrip Patch Antenna dedicated for WSN Applications.

The design and optimization of dual-band patch antennas can be challenging specially in biomedical field, as it involves tuning the antenna's geometry and feed structure to achieve the desired performance over multiple frequency bands. The wearable antennas must meet important requirements including a compact size, a low SAR and a minimal performance degradation under bending. [13] present a performance Analysis of Wearable Dual-Band Patch Antenna Based on EBG and SRR Surfaces. A fully additively manufactured dual band patch antenna operating at 28GHz and 38GHz for 5G/mm wave wearable applications is presented in [14]. In [15] a Dual-band Inset-fed Octagonal Patch Antenna for Wearable Applications is presented. A novel deferentially fed dual-band implantable antenna is proposed for the first time for a fully implantable neuro-microsystem in [16].

In this paper, we propose a dual band patch antenna with a L-Shaped slot and partial ground. The antenna operates at two center frequencies of 2.4 GHz and 3.33 GHz. The antenna shows a good performance which is suitable for biomedical applications.

## 2. Antenna design

### 2.1. calculation method

The first design of our microstrip patch antenna is accomplished by following equations [17]:

✓ **Width of patch ( $W_p$ )**

$$W_p = \frac{C}{2f_r} \sqrt{\frac{2}{\epsilon_r + 1}} \quad (1)$$

Where,

- C: Free space velocity of light.
- $f_r$ : Resonant frequency for the current design.
- $\epsilon_r$ : Dielectric constant of the substrate.

✓ **Effective dielectric constant ( $\epsilon_{eff}$ )**

$$\epsilon_{reff} = \frac{\epsilon_r + 1}{2} + \frac{\epsilon_r - 1}{2} \left[ 1 + \frac{12h}{w} \right]^{-\frac{1}{2}} \quad (2)$$

Where,

- h: Thickness of the substrate

✓ **Length extension**

$$\Delta L = 0.412h \frac{(\epsilon_{reff} + 0.3) \left(\frac{W}{h} + 0.264\right)}{(\epsilon_{reff} - 0.258) \left(\frac{W}{h} + 0.8\right)} \quad (3)$$

✓ **Length of patch (L<sub>p</sub>)**

$$L_p = L_{eff} - 2\Delta L \quad (4)$$

Where,

$$L_{eff} = \frac{C}{2f_r \sqrt{\epsilon_{reff}}} \quad (5)$$

**2.2. Design of the Microstrip Patch Antenna**

The dual band antenna is designed to operate at 2.4 GHz and 3.33 GHz. The size of the antenna is 60 x 55 mm<sup>2</sup>. The substrate used is "Taconic TLX (tm)" with a relative dielectric constant, ε<sub>r</sub> of 2,55, loss tangent, tan δ of 0.0019 and thickness, h of 0.7mm. The feed line technique is introduced to connect the patch to the 50Ω feeding line. W<sub>f</sub> and L<sub>f</sub> are respectively the length and width of the feed line. The ground has been modified and the antenna was introduced partially grounded instead of full ground. The dimensions of partial ground plane are L<sub>G</sub>=57 mm and W<sub>G</sub>=55 mm.

A L-shaped and rectangular slots are inserted in the Patch plane. The slots embedded are illustrated in Fig. 1

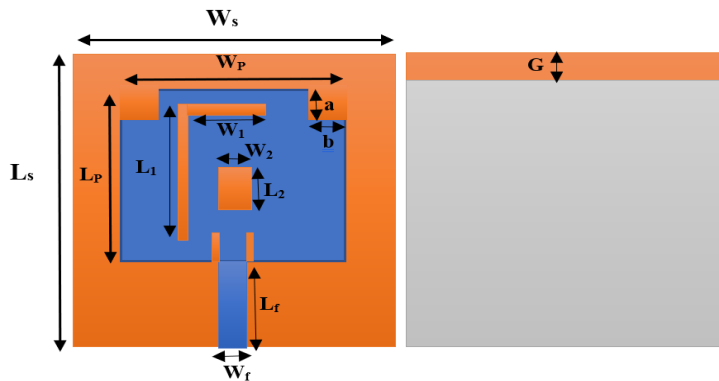


**Fig. 1.** Geometry of proposed Antenna Front view, Back view

The design dimensions of proposed antenna are listed in Table 1.

**Table 1.** Dimensions of the optimized antenna parameters

Parameters	L <sub>S</sub>	W <sub>S</sub>	L <sub>P</sub>	W <sub>P</sub>	L <sub>f</sub>	W <sub>f</sub>	L <sub>1</sub>
Values (mm)	60	55	38	46	15	1.5	32
Parameters	W <sub>1</sub>	L <sub>2</sub>	W <sub>2</sub>	a	b	G	
Values (mm)	15.25	7	5	5	8	3	

### 2.3. Development of the Design

After the dimensions of the initial rectangular patch were finalized, the patch and the ground plane modification were performed to achieve an operating band with enhanced gain, good efficiency, and greater fidelity. The antenna was developed in four stages which are shown in Fig. 2:

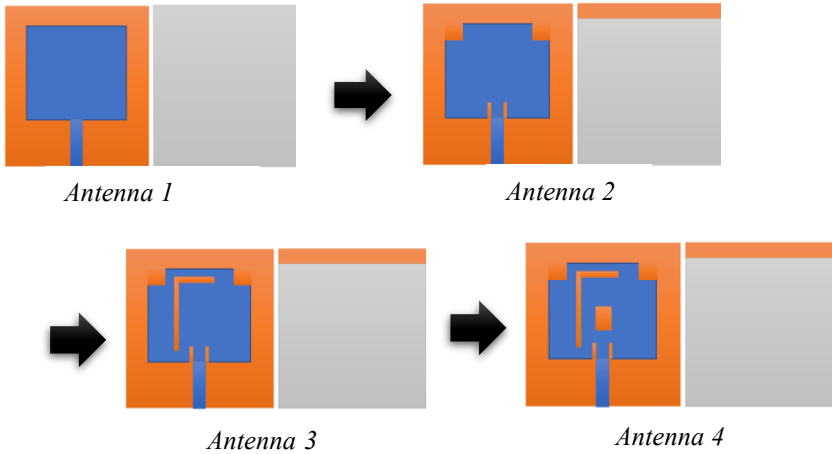


Fig. 2. Evolution process of patch antenna design

### 2.4. Parametric study

The reflection coefficient of different stages is shown in Fig. 3

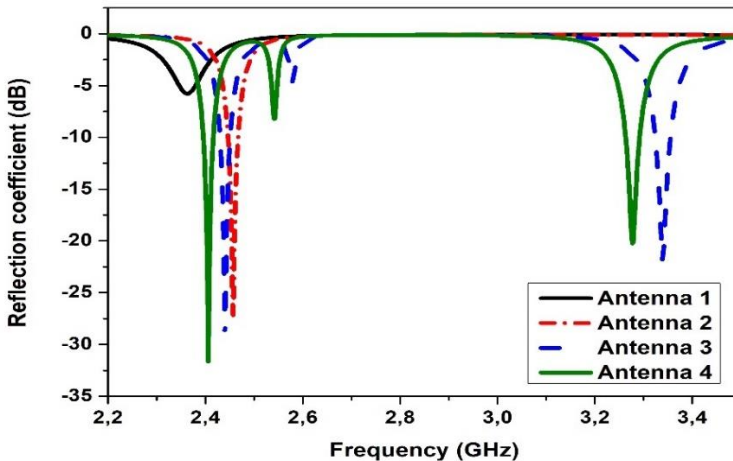


Fig. 3. Analyzed reflection coefficient at different stages

The simulated reflection coefficient ( $S_{11}$ ) for the different stages is shown in Fig. 3. In the first stage, the designed antenna could not achieve any working band due to impedance mismatch and the full ground plane. As for the second stage, an improvement in  $S_{11}$  was observed at 2.4 GHz, due to impedance matching technique by inserting two slots between

the feed line and the patch, in addition to reducing the ground plane length and adding two rectangular slots in the upper sides of the patch. In stage 3, a L-shaped slot is inserted on the patch, the embedded slot has a big role in  $S_{11}$  enhancement, a new working band is observed at 3.38 GHz and the antenna turned from a single-band patch antenna into a dual-band patch antenna. For stage 4 and the final design, a rectangular slot is added in the center of the radioactive element in order to further improve  $S_{11}$ . Consequently, the final antenna model is a good candidate to be used at the designed frequencies.

In general, an L-shaped slot can produce two resonant modes with different resonant frequencies, leading to dual-band operation. The resonant frequencies of the two modes can be adjusted by changing the dimensions of the L-shaped slot, such as the length and width of the slot. In this sense, we made a parametric study for the different dimensions of the added slots.

### i. Analysis of Parameter $L_1$

A parametric analysis of various parameter  $L_1$  values was conducted to obtain appropriate impedance matching. The simulated  $S_{11}$  is presented in Fig. 4, the parameter value was varied between 30 mm and 33 mm in increments of 1 mm. The study revealed that the parameter  $L_1$  had an important influence on the antenna's performances, we obtained the best results with  $L_1=32$  mm.

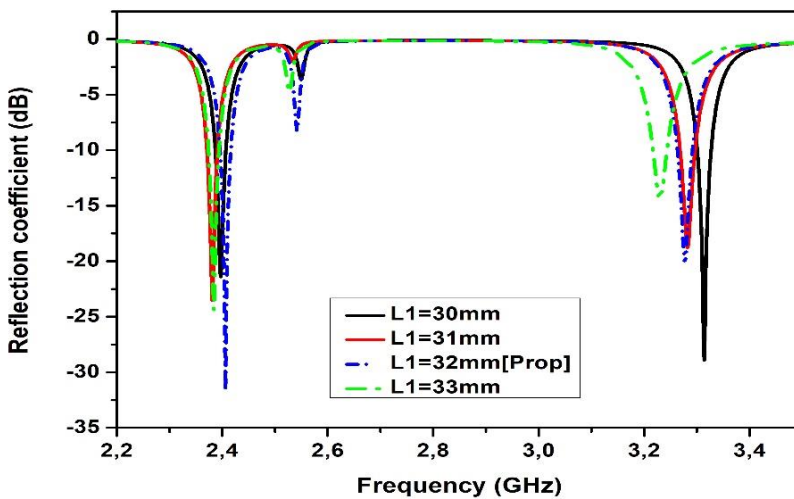


**Fig. 4.** Reflection coefficient with various  $L_1$  values

### ii. Analysis of Parameter $W_1$

In order to analyze the influence of Parameter  $W_1$ , a parametric study was carried out, the Parameter value was varied between 14.25 mm and 17.25 mm in increments of 1 mm. Four results are shown in Fig. 5, the best one is with  $W_1=15.25$  mm. the reflection coefficient was increased from -25 dB to -31.67 dB at 2.4 GHz.

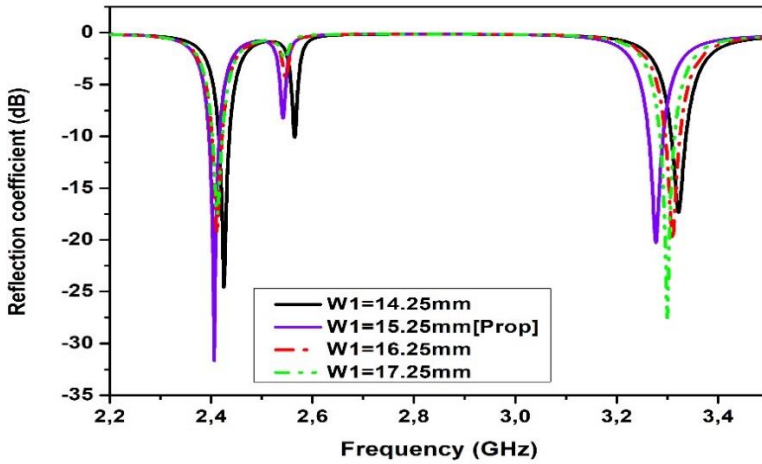


Fig. 5. Antenna reflection coefficient for varied  $W_1$  values

iii. Analysis of Parameter  $L_2$

Another parametric study was performed by changing of  $L_2$  values. The width value was varied between 6 mm and 9 mm in increments of 1 mm. The results are shown in Fig. 6. The variables substantially influenced the antenna return Loss  $S_{11}$ . The value of reflection coefficient is enhanced from -24 dB to -31.67 at 2.4 GHz. The Added slot to the patch modifies the current distribution on the antenna, which improve the return loss.

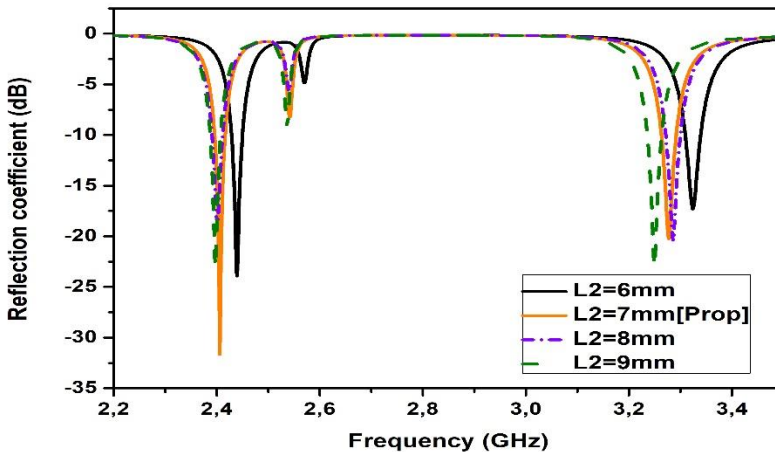


Fig. 6. Reflection coefficient for various  $L_2$  values

iv. Analysis of Parameter  $G$

The impact of the parameter  $G$  on antenna input impedance matching is shown in Fig. 7. The analysis was conducted with varying parameter  $G$ , ranging from 1 to 3 mm in increments of 1 mm. The increase in the parameter  $G$ , lead to a good impedance matching and this explains

the preference of partial ground instead of full ground. The partial ground plane reduces the back radiation of the antenna and help to suppress surface waves that propagate on the ground plane. The best impedance matching is observed with  $G = 3$  mm.

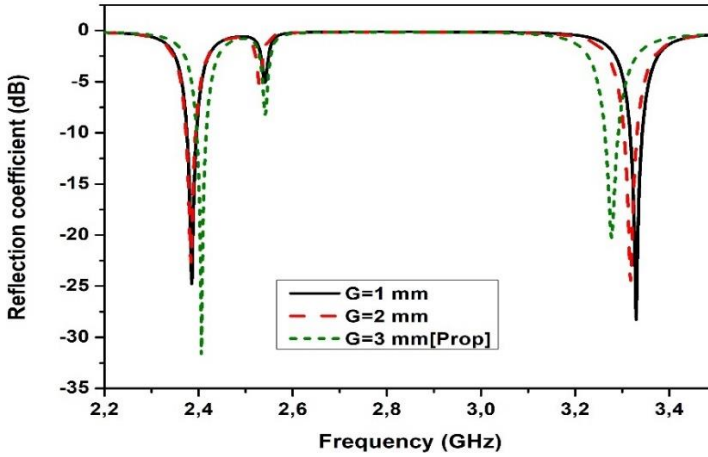


Fig. 7. Reflection coefficient with various G values

### 3. Results and Discussion

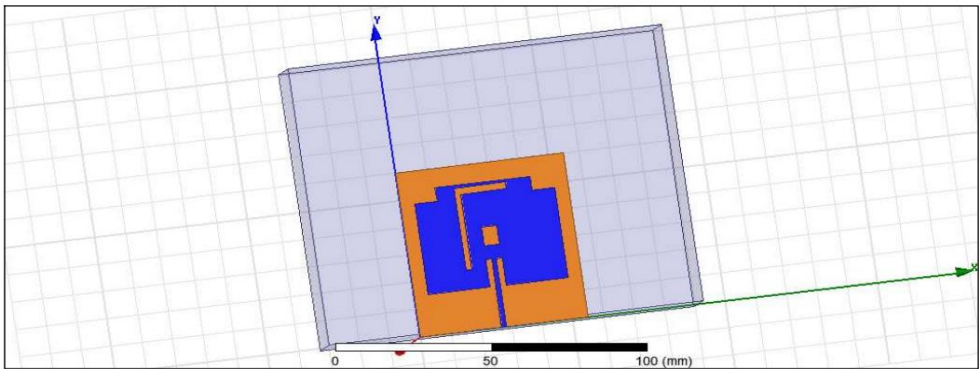
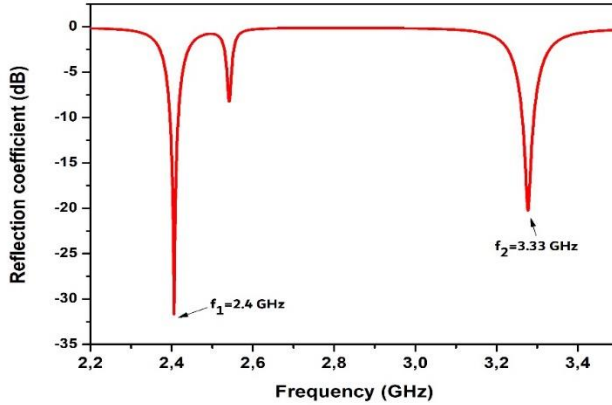


Fig. 8. HFSS boundary setup

#### 3.1. Return loss of proposed antenna

The Return loss of the proposed antenna is represented in the Fig. 9



**Fig. 9.** Analyzed reflection coefficient of proposed structure

The simulated reflection coefficient ( $S_{11}$ ) for the proposed antenna is shown in Fig. 9, The first band appears with a return loss of -31.67 dB, and the second band with a return loss of -20.25 dB.

### 3.2. VSWR

The proposed antenna voltage standing wave ratio (VSWR) simulated curve is illustrated in Fig. 10. The standard values of VSWR are less than 2 for the microstrip patch antenna operating bands. The achieved values of VSWR are 1.08 and 1.16 at 2.4 GHz and 3.33 GHz respectively.

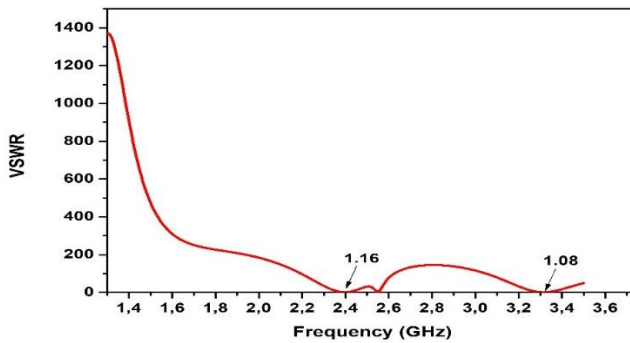


**Fig. 10.** VSWR of proposed structure.

### 3.3. Radiation Pattern

The radiation patterns are revealed in Fig. 11, The gains of proposed work are 5.09 dB and 4.87 dB at 2.4 GHz and 3.33 GHz respectively. The 3D radiation patterns are shown in Fig. 12. Antenna gain relates the intensity of an antenna in a given direction to the intensity that would be produced by a hypothetical ideal antenna that radiates equally in all directions and has no losses.



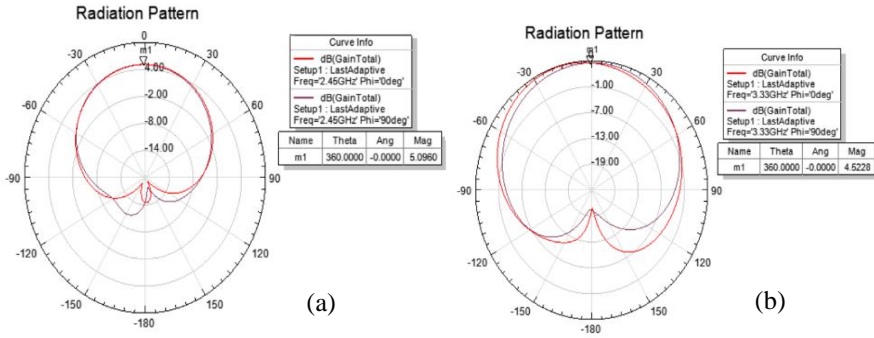


**Fig. 11.** Radiation Pattern of proposed structure;(a) at 2.4 GHz, (b) at 3.33 GHz

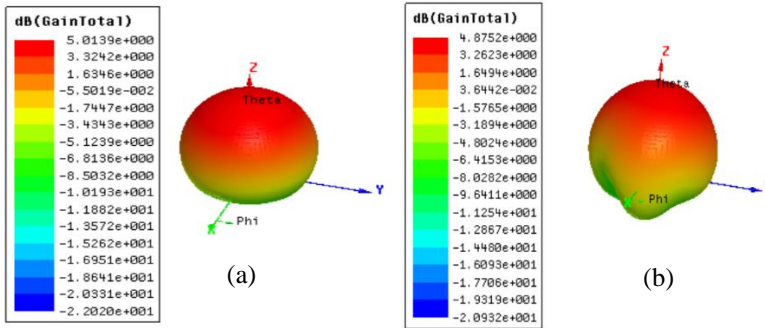


**Fig. 12.** 3D Radiation Pattern of proposed structure;(a) at 2.4 GHz, (b) at 3.33 GHz

Table 2. compare the proposed antenna with other antennas reported in the literature.

**Table 2.** Comparison of proposed antenna with the reported work in literature

Ref.	Freq (GHz)	S <sub>11</sub> (dB)	VSWR	Gain (dB)
[18]	2.41 / 5.8	-14.10 / -27.51	1.49 / 1.08	–
[19]	15.46 / 20.27	≈ - 32 / - 30.2	<2	1.87 / 3.87
[20]	1.875 / 2.4	- 31.6 / - 25.2	<2	5.8 / 4.08
[21]	3.9 / 5.7	-21.55 / -14.73	–	1.27 / 1.35
<b>This work</b>	2.4 / 3.3	-31.67 / -20.25	1.16 / 1.08	5.01 / 4.87

#### 4. Conclusion

This work proposes a dual-band patch antenna with a L-Shaped slot and partial ground, operate at 2.4 GHz and 3.33 GHz, dedicated for biomedical applications. The proposed antenna is a rectangular patch with a L-Shaped and rectangular slots on the patch. The substrate used is "Taconic TLX (tm)" with antenna dimension of  $60 \times 55 \text{ mm}^2$ . With a partial ground plane and slotted patch, the antenna showed a good reflection coefficient of -31.67 dB and -20.25 dB at 2.4 GHz and 3.27GHz respectively. The L-shaped slot added on the patch produce two resonant modes with different resonant frequencies and it has been demonstrated that the partial ground improves clearly the antenna performances specifically the return loss. The antenna showed also a high gain of 5.09 dB at 2.4 GHz, which is Suitable for biomedical applications. For more further experiments of proposed antenna, the SAR and the link budget calculations can also be done in future.

## Conflict of interest

There is no conflict of interest for this study.

## References

1. A. Ahmad, F. Faisal, S. Ullah, and D.-Y. Choi, *Appl. Sci.* **12**, 9218 (2022)
2. S. S. Ojha, P. K. Singhal, and V. V. Thakare, *Meas. Sens.* **24**, 100532 (2022)
3. L. G. Ayalew and F. M. Asmare, *Heliyon* **8**, e12030 (2022)
4. D. Sarkar, K. Saurav, and K. V. Srivastava, (2013)
5. K. K. Parashar, V. K. Singh, and R. Tiwari, (2014)
6. A. Sid, P.-Y. Cresson, N. Joly, F. Braud, and T. Lasri, *AEU - Int. J. Electron. Commun.* **157**, 154412 (2022)
7. P. Shirvani, F. Khajeh-Khalili, and M. H. Neshati, *AEU - Int. J. Electron. Commun.* **138**, 153840 (2021)
8. M. Al-Hasan, P. R. Sura, A. Iqbal, J. J. Tiang, I. B. Mabrouk, and M. Nedil, *AEU - Int. J. Electron. Commun.* **138**, 153896 (2021)
9. G. Singla, R. Khanna, and D. Parkash, *Int. J. Microw. Wirel. Technol.* **11**, 523 (2019)
10. M. A. M. Said, S. M. I. N. S. Jaya, Z. Zakaria, M. H. Misran, and M. M. Ismail, *Bull. Electr. Eng. Inform.* **10**, 3265 (2021)
11. A. Wei, (2013)
12. R. George and T. Anita Jones Mary, in *2021 Int. Conf. Adv. Electr. Comput. Commun. Sustain. Technol. ICAECT* (IEEE, Bhilai, India, 2021), pp. 1–6
13. A. Wajid, A. Ahmad, S. Ullah, D. Choi, and F. U. Islam, *Sensors* **22**, 5208 (2022)
14. K. Hu, Y. Zhou, S. K. Sitaraman, and M. M. Tentzeris, in *2022 IEEE Int. Symp. Antennas Propag. USNC-URSI Radio Sci. Meet. AP-SURSI* (IEEE, Denver, CO, USA, 2022), pp. 878–879
15. S. Mahapatra, J. Mishra, and M. Dey, in *Adv. Intell. Comput. Commun.*, edited by S. Das and M. N. Mohanty (Springer Singapore, Singapore, 2021), pp. 699–706
16. Z. Duan, Y.-X. Guo, R.-F. Xue, M. Je, and D.-L. Kwong, *IEEE Trans. Antennas Propag.* **60**, 5587 (2012)
17. A. D. Dhumale, (2018)
18. S. Küçükcan and A. Kaya, *Eur. J. Sci. Technol.* (2022)
19. M. M. Islam, M. T. Islam, and M. R. I. Faruque, *Sci. World J.* **2013**, 1 (2013)
20. N. Dorairajan and C. M. Perumal, *Wirel. Netw.* **26**, 5883 (2020)
21. R. Roy, A. Singh, O. P. Kumar, T. Ali, and M. Pai M. M., *Bull. Electr. Eng. Inform.* **9**, 1477 (2020)